Geometrical Scaling Limits of Heat-Assisted Magnetic Recording

Stephanie Hernandez[1], Zengyuan Liu[1], Peiran Jin[1], Steven D. Granz[1], Pavol Krivosik[2], Raman Venkataramani[3], William Radich[3], Tim Rausch[1], John Dykes[1], and Edward C. Gage[1]

[1]Seagate Research, Seagate Technology, Shakopee, MN 55379 USA
[2]Recording Head Operations, Seagate Technology, Bloomington, MN 55435 USA
[3]VLSI Channels, Seagate Technology, Longmont, CO 80503 USA

System-level requirements for heat-assisted magnetic recording at high areal density are presented in this article. The primary factors that affect bit error rate (BER) are spatial, or media, signal-to-noise ratio (SNR), reader SNR, and channel bit density (CBD). Spatial SNR is largely determined by the interaction between the writer properties and the media properties. For example, how well the thermal gradient matches the grain size. Spatial SNR also depends on how well the reader cross-track resolution matches the track pitch, and the quality of the written pattern. For any given level of spatial SNR, there exists a combination of CBD and reader SNR that results in the desired level of performance. This article elucidates some of the tradeoffs that may be needed to maintain BER as areal density increases, for different bit aspect ratio scenarios. For very high areal density, we show that the geometrical requirements are extremely aggressive, which will most likely require significant invention in head and drive architecture design.

Index Terms— **Heat-assisted magnetic recording (HAMR), micromagnetic modeling, recording subsystems.**

I. Introduction

THE hard disk drive (HDD) industry is at the cusp of significant change: the first products based on energy assist methods [1], [2] have been announced and planned for release in the near future. Energy assist methods aim to address the so-called magnetic recording trilemma, which states that in order to maintain the signal-to-noise ratio (SNR) of HDD systems as bit sizes decrease, the media grain diameter must also decrease. If that is the case, materials with high magnetocrystalline anisotropy must be used in order to maintain thermal stability. Heat-assisted magnetic recording (HAMR) [3] employs a heat source during the write process to quickly and efficiently reduce the energy barrier of the recording medium. This technology has enabled the development and use of FePt-based media materials. In addition to high anisotropy, very small grain sizes have been demonstrated in this type of magnetic recording media [4].

Recent HAMR spin-stand demonstrations stand at around 2.45 Tb/in^2 [5]. These feature state-of-the-art heads and media, aggressive head-disk clearance, and advanced drive architectures such as interlaced magnetic recording (IMR). An ongoing research effort [6], [7] exists to elucidate the ultimate areal density capability (ADC) of HAMR systems. The Advanced Storage Technology Consortium HDD Roadmap includes HAMR as the main successor to perpendicular magnetic recording with an ADC limit of around 4–5 Tb/in^2 according to estimates obtained from academic and industrial research [7]–[9].

Previously published efforts to quantify HAMR system requirements as a function of ADC [9] have focused on quantifying the media properties required in order to maintain an assumed level of spatial SNR. In this article, we highlight the contribution of the readback process: the reader SNR and resolution required depend strongly on the media SNR the write process is able to deliver. To do so, a micromagnetic system model is employed. Bit error rate (BER) is the primary metric used to evaluate the performance of the different system scenarios. The primary factors that influence BER are the system SNR, and the channel bit density (CBD). Total system SNR may be decomposed into spatial, or written-in, SNR, and reader SNR. Spatial noise is what is commonly referred to as media noise. Nonetheless, it is not only determined by the media properties, but also by their interaction with the recording head properties. Spatial SNR may be further partitioned into transition SNR and remanence SNR [10]. Transition noise, or jitter, is a dominant noise source in HAMR, and much research has been performed in recent years to understand and mitigate it [11]–[13]. Reader SNR is associated with the signal produced, and the noise sources present, during the readback process. The signal produced by the reader is determined by the average response of the reader's active element to the media pattern. Reader noise is primarily composed of thermal magnetics noise, but also includes electronics noise such as shot noise and Johnson noise [14], [15]. As ADC increases, the necessary reduction in bit size, reader geometry, and writer geometry will unavoidably lead to an exacerbation of all of these noise sources. Non-linear distortions, which are shifts in the transition locations in the time domain, may also contribute to BER. However, through an analysis similar to the one described in [16], we find that distortions represent a small portion of the errors observed in the simulations performed in this analysis. A deeper analysis of non-linear transition shift at high linear density is beyond the scope of this work, but it nevertheless warrants further discussion in a future publication.

Manuscript received August 2, 2020; revised November 6, 2020; accepted November 16, 2020. Date of publication November 25, 2020; date of current version February 18, 2021. Corresponding author: S. Hernandez (e-mail: stephanie.hernandez@seagate.com).

Color versions of one or more figures in this article are available at https://doi.org/10.1109/TMAG.2020.3040497.

Digital Object Identifier 10.1109/TMAG.2020.3040497

0018-9464 © 2020 IEEE. Personal use is permitted, but republication/redistribution requires IEEE permission.
See https://www.ieee.org/publications/rights/index.html for more information.

Authorized licensed use limited to: Seagate Technology. Downloaded on June 07,2021 at 16:01:03 UTC from IEEE Xplore. Restrictions apply.

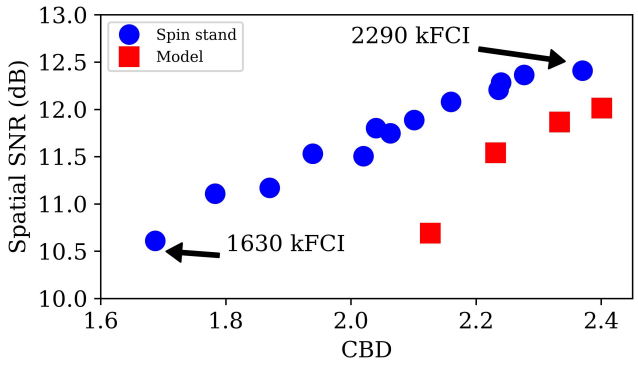

Fig. 1. Spatial SNR versus CBD for model and experiment.

CBD is a measure of the down-track resolution of the system, which is defined as

$$\text{CBD} = \text{PW50/BL} \tag{1}$$

where PW50 is the full width half maximum (FWHM) of dS_{trans}/dx (the derivative in the down-track direction x of the signal in the vicinity of a transition S_{trans}), and BL is the bit length in the down-track direction. Simplistically, CBD is a measure of how many bits the reader can resolve in the down-track direction. A system with higher CBD should require a higher SNR to achieve the same BER: the channel requires more signal to deconstruct the greater intersymbol interference present in the system. Fig. 1 illustrates this concept. It shows spin-stand measurements and micromagnetic modeling where the laser power has been optimized to achieve a BER of -2.0 dec at a track density of 650 kTPI. CBD was varied by varying the linear density within the values noted in the figure. Spatial SNR in both the measurement and the model is obtained as described in [10]. The modeling methodology will be explained in Section II; however, the modeled heads and media are similar to those used in the measurement. The figure shows that for a roughly 650 kFCI increase in linear density, a 2.5 dB improvement in spatial SNR is required to maintain the same level of performance.

This article aims to shed light on the tradeoffs required to maintain a reasonable level of performance as both linear density and track density increase. The BER of a system is mostly determined by its spatial SNR, reader SNR, and CBD. With that in mind, we will demonstrate that there should be two main aspects to HAMR system design. First, spatial SNR should be maximized via intelligent design of heads and media, and their interaction. And second, at a given spatial SNR, the reader SNR and down-track resolution (i.e., CBD) required for BER maintenance may be determined. In other words, if spatial SNR cannot be improved or maintained, the reader SNR and CBD need to make up for this. Conversely, if reader SNR decreases and CBD increases, spatial SNR must be improved.

II. Modeling Methodology

The HAMR recording process is modeled using the renormalized Landau–Lifshitz–Gilbert (LLG) method [17], which is often used to simulate high-temperature magnetization dynamics. This method allows the usage of cell sizes larger than atomic length scales by estimating the change in magnetic properties as a function of temperature. The cell size used in the simulations presented in this article is $1.5 \times 1.5 \times 1.5$ nm^3. A Voronoi grain structure is overlaid on the medium grid in the in-plane direction to simulate the irregular grain structure of real HAMR media. The average grain diameter is varied in the modeling performed for this study, while the standard deviation in grain size is set at around 15%. The model assumes media magnetic properties typical to those of FePt, and similar to those of [10].

A typical HAMR head features a near field transducer (NFT) that serves as the heat source and provides a very concentrated thermal spot within the media. This thermal spot has a size, shape, and temperature gradient that are determined by the properties of the NFT and its interaction with the media optical and thermal properties. In other work [10], [18], [19], and for the modeling shown in Fig. 1, the thermal spots utilized are based on real NFT designs. However, for most of the modeling presented in this article, thermal profiles are artificially engineered to have the properties necessary for a reasonable level of performance in conjunction with the other conditions considered. Magnetic fields are assumed uniform in both magnitude and angle, and both values may also be optimized at the different ADC conditions.

Pseudorandom bit sequences (PRBS) are written on 50 unique media sections, with a length of 31 bits. The generator polynomial is $x^5 + x^3 + 1$, which produces the following PRBS: 1111100011011010100000100101100. In some of the cases presented in the Sections III and IV, one isolated track is studied. In others, two tracks are written on either side of the track of interest with patterns that are random and uncorrelated relative to the PRBS and each other. The micromagnetic readback process consists of quasi-static LLG simulations of a reader flying over media maps containing the patterns produced during the write process. The reader is divided into a grid of $2 \times 2 \times 2$ nm^3 cells, thereby capturing any non-uniformities that may be present in the reader response to the media fields. Reader properties, such as reader width, shield-to-shield spacing, and clearance are varied and optimized to achieve the desired level of performance. Subsequently, an ensemble waveform analysis, as described in [10], is employed to extract the spatial SNR and CBD values quoted in the following sections. The channel model described in [20] is used to calculate BER from the PRBS waveforms. The micromagnetically modeled patterns contain only spatial noise. White noise, representing the time-based random fluctuations present in the readback signal, must be added to the modeled waveforms. The level of white noise is estimated from the average signal of the modeled readback waveforms and the required level of reader SNR to achieve a given BER threshold. Given this assumed level of reader SNR, the magnitude of the additive noise (N) is expressed as

$$N = S\sqrt{\text{OSR/BW}} \times 10^{\text{ReaderSNR}/20} \tag{2}$$

where S is the rms signal calculated from the simulated waveforms, OSR is the oversampling ratio, and BW is the bandwidth. OSR represents the number of samples per bit and

Authorized licensed use limited to: Seagate Technology. Downloaded on June 07,2021 at 16:01:03 UTC from IEEE Xplore. Restrictions apply.

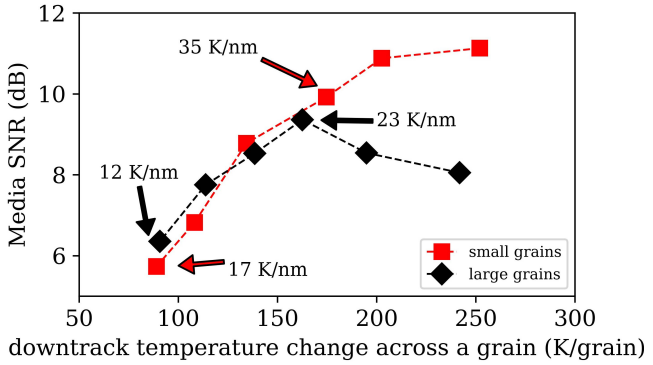

Fig. 2. Media SNR as a function of thermal gradient expressed as change in temperature across the width of a grain for two different grain sizes (5 and 7.5 nm). The arrows represent the actual thermal gradient values in K/nm for the points highlighted.

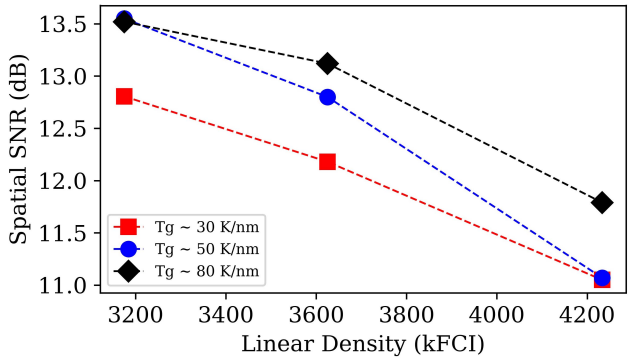

Fig. 3. Spatial SNR as a function of linear density for different thermal gradient scenarios.

is equal to 7 in this study. A low-pass filter is applied to remove unnecessary high-frequency content with a cutoff frequency equal to BW multiplied by frequency of the shortest mark in the PRBS. In this work, BW = 1.0. The reader SNR values quoted depend strongly on BW; however, the offset in SNR should be consistent between different values, and simple to convert if required.

The metrics of interest in this study are the following: thermal gradient (T_G), thermal width (T_W), grain size, reader down-track resolution (PW50), CBD, reader cross-track resolution (CT10), reader SNR, spatial SNR, and BER. T_G is the temperature gradient as measured at the transition position, which is assumed identical in both the down-track and the cross-track directions. T_W is the width of the thermal profile at 50% of the maximum temperature. The magnetic field is assumed to be in the range of 0.8–1.0 T with a 45° angle relative to the media plane. CT10 is the width of the reader response to a point charge in the cross-track direction at 10% of the maximum signal. PW50 and CBD were defined in Section I. Unless otherwise stated, the results presented in the following sections employ the procedure outlined above to extract spatial SNR and BER.

III. Head and Media Contributions to Spatial SNR and BER

The interaction between the media and the writer is what predominately determines the spatial SNR of the system. Much research has gone into the development of future recording head designs, in addition to media design. The goal in head design development is to continually improve performance, while at the same time maintaining reliability [21]. The thermal gradient (T_G) in the down-track direction is one of the most important metrics that define how well bit transitions are written. Fig. 2 shows media SNR as a function of the down-track thermal gradient over the grain diameter, for two chosen grain diameters, obtained from micromagnetic modeling. Single-tone patterns are recorded on 50 unique randomly generated media instances at a track width large enough not to result in an SNR degradation when larger grains are used. Media SNR is calculated directly from the resulting magnetization patterns as described in [12]. By scaling the shape and width of the thermal profile, the thermal gradients shown in the figure are obtained, at a similar track width for all of the data points. Fig. 2 illustrates the importance of the thermal gradient on media SNR, and suggests that, all other factors being equal, bit quality may be entirely dependent on what the thermal gradient is relative to the grain size. Roughly the same SNR is obtained for two different grain sizes at the same rate of temperature change across the length of a grain. The arrows illustrate that, even though the rate of temperature change across a grain is the same for the two cases, the actual thermal gradient values in K/nm are quite different. Also, for large grains, a plateau in SNR, and a subsequent decrease, are observed as the thermal gradient increases. In this case, it might be possible that grains are not spending enough time at temperatures that allow sufficient spontaneous magnetization to be susceptible to the applied magnetic fields.

Single-track spatial SNR extracted from an ensemble waveform analysis as described in Section II as a function of linear density for different thermal gradient scenarios is shown in Fig. 3. The average grain size is 5 nm, and the written track width is close to 20 nm for all cases presented. As linear density increases, there is an expected decrease in SNR from the reduction in bit size and, consequently, number of grains per bit. As linear density increases, the gain from increasing thermal gradient increases, and the larger the thermal gradient required to see any improvement in performance. Figs. 2 and 3 demonstrate that while thermal gradient is a key parameter in determining spatial SNR, improving it will not result in a performance gain if the media and the recording conditions are not optimized along with it.

Triple track spatial SNR as a function of CT10 (as defined in Section II), normalized to the track pitch (TP), for two different track density scenarios is shown in Fig. 4. The areal density is 4.1 Tb/in^2, and while the width of the thermal profiles is different to match each track density, T_G is constant for both cases. Actual CT10 values range from 17.4 to 25.2 nm. The optimal CT10/TP seems to shift toward CT10/TP = 1 with increasing track density. As CT10 increases beyond TP, more of the adjacent tracks are sensed by the reader, resulting in an SNR degradation. This demonstrates that the CT10 can be carefully chosen to optimize the spatial SNR, keeping in mind that narrower CT10 can only be achieved by decreasing the physical cross-track dimension of the reader element. This will

Authorized licensed use limited to: Seagate Technology. Downloaded on June 07,2021 at 16:01:03 UTC from IEEE Xplore. Restrictions apply.

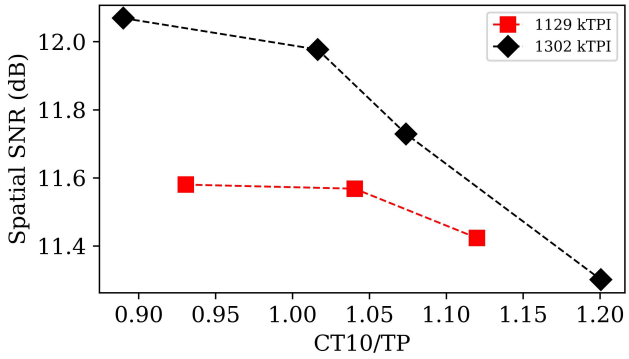

Fig. 4. Triple track spatial SNR as a function of reader cross-track resolution (normalized to the TP), for different track densities at 4 Tb/in^2.

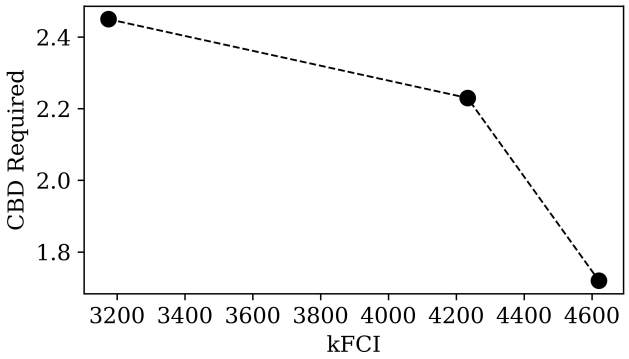

Fig. 5. CBD required to maintain a BER of −1.8 as a function of linear density assuming a single wide isolated track.

TABLE I
SYSTEM SCENARIOS FOR 2.4, 4.1, AND 6.0 TBPSI ADC TARGETS

ADC (Tbpsi)	2.4				4.1				6
Bit Aspect Ratio	2.8		3.1		2.8		3.2		3
Linear Density (kFCI)	2619		2764		3175		3625		4233
Track Density (kTPI)	935		887		1303		1129		1417
Bit length (nm)	9.7		9.25		8.0		7.0		6.0
Track pitch (nm)	27		28.6		19.5		22.5		17.9
grain size (nm)	6.5		6.5		5.1		5.1		5.1
Thermal Width (nm)	35.0		35.0		25.0		25.0		20.0
Thermal gradient (K/nm)	17.0		20.2		30.0		32.0		50.0
CT10/TP	1.11		1.05		1.02		0.97		0.97
CBD	2.25	2.53	2.39	2.59	1.94	2.29	1.95	2.3	2.08
PW50 (nm)	21.8	24.5	22.1	24.0	15.5	18.3	13.7	16.1	12.5
Reader SNR (dB)	16.0	18.0	19.0	23.0	22.0	24.0	19.0	22.0	24.0
Spatial SNR (dB)	12.71		12.2		11.81		11.58		9.32

undoubtedly lead to increased reader noise and consequently reduced system performance.

Fig. 5 shows the CBD required to maintain a BER of –1.8, for single isolated tracks written at different linear densities with the same writer and media combination. The CBD requirements increase significantly as a function of linear density, due to both the increase in linear density and the reduction in spatial SNR that occur as BLs decrease. This demonstrates that it is crucial to examine different ways to improve the spatial SNR as ADC increases.

IV. HAMR SYSTEM REQUIREMENTS AT HIGH ADC

The different system scenarios shown in Table I are obtained by optimizing the thermal profile properties (T_W, T_G), media properties (grain size), and reader properties (CT10, P50, and reader SNR) in order to maintain a BER of –2.0 dec. Triple track recording is performed by optimizing the peak temperature of the thermal profile in order to maximize pattern quality, while at the same time minimizing adjacent track interference effects. Spatial SNR from ensemble waveform analysis is shown at the bottom of the table. Two bit aspect ratio (BAR) scenarios are included for 2.4 and 4.0 Tb/in^2. In general, higher BAR results in increased thermal gradient requirements as BLs decrease and transition quality becomes more important. CT10 values close to the TP are, in general, best for optimization of spatial SNR. CBD and reader SNR are varied to elucidate the tradeoffs required to maintain a similar level of performance. As stated previously, when CBD increases, due to either increasing linear density or increasing PW50, higher SNR is required to maintain BER. Roughly 0.05–0.15 CBD inflation results in a 1-dB reader SNR requirement increase. At higher BAR, it is more difficult to maintain spatial SNR, even when T_G is high. That fact, coupled with the higher linear density, results in more stringent P50 and reader SNR requirements. A 6 Tb/in^2 scenario is also included to convey the dramatic increase in system requirements at such high ADC. We have, however, employed conventional magnetic recording (CMR) in all of the scenarios considered in Table I. It may be possible that more advanced recording schemes such as shingled magnetic recording (SMR) and IMR [5], or improved channel architectures [22] would lead to a relaxation of some of these requirements at high ADC.

V. CONCLUSION

This work presents the system-level requirements for high ADC HAMR systems, and some of the potential tradeoffs that may be made to maintain performance with increasing areal density. BER strongly depends on the level of spatial SNR the system is able to achieve. This suggests that head and media design must prioritize optimization of spatial SNR, and the modeling presented in this article demonstrates that this is only achieved if the head and media properties are well matched. For a given level of spatial SNR, the down-track reader resolution (CBD) and SNR may be optimized to achieve the desired level of performance. In other words, if the spatial SNR level is low, CBD and reader SNR must be improved, and vice versa. Also, if CBD increases with ADC, the reader SNR may be improved for BER maintenance, and vice versa. As ADC increases, the requirements become much more stringent. This will necessitate either a significant reduction in head geometries or invention in design or materials that achieve the resolution requirements outlined here. Also, if the requirements outlined in this article cannot be achieved, drive and channel architecture advances may lead to a relaxation of these requirements.

REFERENCES

[1] *Earnings Call*, Seagate, Cupertino, CA, USA, Feb. 2020.
[2] *Earnings Call*, Western Digital, San Jose, CA, USA, Jan. 2020.
[3] M. H. Kryder *et al.*, "Heat assisted magnetic recording," *Proc. IEEE*, vol. 96, no. 11, pp. 1810–1835, Nov. 2008.

Authorized licensed use limited to: Seagate Technology. Downloaded on June 07,2021 at 16:01:03 UTC from IEEE Xplore. Restrictions apply.

[4] Y. Kabota *et al.*, "Heat-assisted magnetic recording's extensibility to high linear and areal density," *IEEE Trans. Magn.*, vol. 54, no. 11, Nov. 2018, Art. no. 3201206.
[5] S. Granz *et al.*, "Areal density comparison between conventional, shingled, and interlaced heat-assisted magnetic recording with multiple sensor magnetic recording," *IEEE Trans. Magn.*, vol. 55, no. 3, pp. 1–3, Mar. 2019.
[6] C. Rea *et al.*, "Areal density limits for HAMR and PMR," *IEEE Trans. Magn.*, vol. 52, no. 7, Feb. 2016, Art. no. 3001304.
[7] D. Suess, *HAMR System Requirements at 4 Tbpsi*. Austin, TX, USA: TMRC, 2019.
[8] C. Vogler, C. Abert, F. Bruckner, D. Suess, and D. Praetorius, "Areal density optimizations for heat-assisted magnetic recording of high-density media," *J. Appl. Phys.*, vol. 119, Jan. 2016, Art. no. 223903.
[9] D. Weller *et al.*, "A HAMR media technology roadmap to an areal density of 4 Tb/in^2," *IEEE Trans. Magn.*, vol. 50, no. 1, Jan. 2014, Art. no. 3100108.
[10] S. Hernández *et al.*, "Using ensemble waveform analysis to compare heat assisted magnetic recording characteristics of modeled and measured signals," *IEEE Trans. Magn.*, vol. 52, no. 2, Sep. 2016, Art. no. 3000406.
[11] K. Kim and J. Moon, "Experimental characterization of transition noise in HAMR," *IEEE Trans. Magn.*, vol. 49, no. 7, pp. 3675–3678, Jul. 2013.
[12] J.-G. Zhu and H. Li, "Understanding signal and noise in heat assisted magnetic recording," *IEEE Trans. Magn.*, vol. 49, no. 2, pp. 765–772, Feb. 2013.
[13] Y. Dong and R. H. Victora, "Micromagnetic study of medium noise plateau," *IEEE Trans. Magn.*, vol. 45, no. 10, pp. 3714–3717, Oct. 2009.
[14] Y. Chen *et al.*, "2 Tbit/in2 reader design outlook," *IEEE Trans. Magn.*, vol. 46, no. 3, pp. 698–701, May 2010.
[15] O. Heinonen and H. S. Cho, "Thermal magnetic noise in tunneling readers," *IEEE Trans. Magn.*, vol. 40, no. 4, pp. 2227–2232, Jul. 2004.
[16] N.-H. Yeh, Z. Zhang, and P. Steiner, "From component SNR to system SFR," *IEEE Trans. Magn.*, vol. 48, no. 11, pp. 3899–3902, Nov. 2012.
[17] R. H. Victora and P.-W. Huang, "Simulation of heat-assisted magnetic recording using renormalized media cells," *IEEE Trans. Magn.*, vol. 49, no. 2, pp. 751–757, Feb. 2013.
[18] S. Hernandez, P. Krivosik, P.-W. Huang, W. R. Eppler, T. Rausch, and E. Gage, "Parametric comparison of modeled and measured heat-assisted magnetic recording using a common signal-to-noise metric," *IEEE Trans. Magn.*, vol. 52, no. 7, pp. 1–4, Jul. 2016.
[19] S. Hernández *et al.*, "Data rate effects in heat assisted magnetic recording," *IEEE Trans. Magn.*, vol. 53, 2017, Art. no. 8205104.
[20] R. Venkataranmani, "Integrated near field transducer heat assisted magnetic recording head: Design and recording demonstration," U.S. Patent 8 737 460, 2009.
[21] A. V. Itagi *et al.*, "Integrated near field transducer heat assisted magnetic recording head: Design and recording demonstration," in *Proc. Optical Data Storage Top. Meeting*, 2009, pp. 1–4.
[22] L. Kong *et al.*, "A detector-aware LDPC code optimization for ultra-high density magnetic recording channels," in *Proc. Intermag Conf.*, Apr. 2018, p. 1.

Authorized licensed use limited to: Seagate Technology. Downloaded on June 07,2021 at 16:01:03 UTC from IEEE Xplore. Restrictions apply.